

Quantifying Wildfire-Induced Impacts to Photovoltaic Energy Production in the western United States

Samuel D. Gilletly, Nicole D. Jackson, and Andrea Staid
Sandia National Laboratories, Albuquerque, New Mexico, 87123, USA

1 **Abstract**—Smoke from wildfires results in air pollution that can
2 impact the performance of solar photovoltaic plants. Production
3 is impacted by factors including the proximity of the fire to
4 a site of interest, the extent of the wildfire, wind direction, and
5 ambient weather conditions. We construct a model that quantifies
6 the relationships among weather, wildfire-induced pollution, and
7 PV production for utility-scale and distributed generation sites
8 located in the western United States. The regression model iden-
9 tified a 9.4%–37.8% reduction in solar PV production on smoky
10 days. This model can be used to determine expected production
11 losses at impacted sites. We also present an analysis of factors that
12 contribute to solar photovoltaic energy production impacts from
13 wildfires. This work will inform anticipated production changes
14 for more accurate grid planning and operational considerations.

15 **Index Terms**—air quality, wildfires, particulate matter, PM2.5,
16 solar PV generation

I. INTRODUCTION

19 Wildfire incidents are increasing in both frequency and
20 size throughout much of the western United States [1]. A
21 consequence of these incidents is the reduction in air quality
22 due to increases in dust and other aerosols [2] as well as fine
23 particulate matter concentrations [3] [4], even when account-
24 ing for seasonal fluctuations [5]. This is concerning not only
25 for the livelihood of those impacted, but also when it comes
26 to considerations of power grid planning and operations.

27 The fast-growing solar industry in the western United States
28 (U.S.) plays a large role in electricity production, making wild-
29 fire impacts particularly concerning. California, for example,
30 produced 14.2% of in-state electricity with solar photovoltaics
31 (PV) and solar thermal plants in 2019 [6], and at least 50% of
32 its energy is expected to be generated from solar sources in
33 the coming decades [7]. For the period 2013–2017, California
34 annually averaged 8,143 fires and 897,146 burned acres [8].
35 Therefore, it is crucial that grid operators can plan for these
36 production impacts to better manage resources during what are
37 already some of the most vulnerable times for the electricity
38 sector.

39 Solar energy production is particularly vulnerable to the
40 wide-reaching second-order effects of wildfires. Smoke from
41 large fires can travel a considerable distance, bringing with
42 it pollution in the form of small particulate matter that ob-
43 structs solar radiation and thus PV energy production [9].

This work was funded by the U.S. Department of Energy's Advanced Grid Modeling Research Program.

Prior work linking air quality to PV performance has been
44 broadly focused on ambient aerosols and is either based on
45 experimental field data [10], laboratory tested modules [11], or
46 global computational models [12]. Ambient aerosols have
47 been estimated to reduce utility-scale PV generation in Korea
48 by 15–24% [13]. Experimental testing of module performance
49 during a wildfire event in Spain resulted in average reduction
50 of 34% [14]. Small PM2.5 particles (fine particulate matter of
51 2.5 microns or less in diameter) are the primary pollutant in
52 wildfire smoke [15]. Our work presented here seeks to build
53 on these prior efforts by analyzing the impact of PM2.5 due to
54 wildfires on utility-scale and distributed PV energy generation
55 in field-collected data. By understanding the factors that im-
56 pact production and the degree to which energy production is
57 reduced from wildfires, we can provide better predictive tools
58 for grid planning, thus minimizing costs for grid operators
59 during and after wildfire events. In addition, site owners and
60 operators will be better able to quantify expected losses for
61 improved site management.

62 Here, we present an analysis with the goal to quantitatively
63 understand the relationships among weather, wildfire-induced
64 pollution, and PV production. To do so, we analyze historical
65 production data from a series of PV plants located in the
66 western U.S. as well as daily particulate matter and weather
67 data. The available production data for many sites overlap with
68 two major wildfire events from 2018: the Mendocino Com-
69 plex fire during July–September; and the Camp Fire during
70 November. The Mendocino Complex Fire was comprised of
71 the Ranch and River fires and resulted in the combined burning
72 of 459,123 acres [16], [17]. Similarly, the Camp Fire burned
73 153,336 acres [18]. These fires were near the average annual
74 number of burned acres for the previous five years. While
75 these fires originated in California, they affected much of the
76 western United States. Below, we describe our data fusion
77 process, statistical approach, and resulting predicted solar PV
78 energy production model to understand impacts from wildfire-
79 related PM2.5.

II. METHODS

80 The evaluation of wildfire-related PM2.5 in this analysis is
81 driven by production, weather, and particulate matter for solar
82 PV sites located in the western United States. Details regarding
83 the datasets used, data processing, and data analysis activities
84 are provided in the following subsections.

87 **A. Data**

88 We combine historical solar PV energy production data with
 89 weather and pollution data with the goal of understanding the
 90 impact that nearby wildfires have on site production. This work
 91 relies on using diverse datasets, which results in a mismatch
 92 in resolutions. Here, we described the datasets used in more
 93 detail.

94 *1) Production Data:* The utility-scale production data used
 95 in the study is provided by Sandia's PV Reliability, Operations
 96 & Maintenance (PVROM) database [19]. This repository con-
 97 tains production, operations, and maintenance data from 800+
 98 sites located in the United States. Production data includes
 99 time series data for the power and energy generated. Site-level
 100 meteorological variables such as plane-of-array irradiance,
 101 ambient temperature, module temperature, and wind speed are
 102 also available. For this project, we subset PVROM to sites in
 103 Arizona, California, Idaho, Oregon, and Utah, and limit the
 104 data to April 2018 - July 2019 period. Additional eligibility
 105 was based on the availability of historical production that
 106 overlapped with the Mendocino Complex and Camp Fires as
 107 well as proximity to PM2.5 monitoring stations. These criteria
 108 resulted in 68 eligible sites for analysis: 52 utility-scale sites;
 109 and 16 distributed sites (see Figure 1 for distribution of site
 110 sizes in terms of DC kW). These sites contained over 20,000
 111 days of production data.

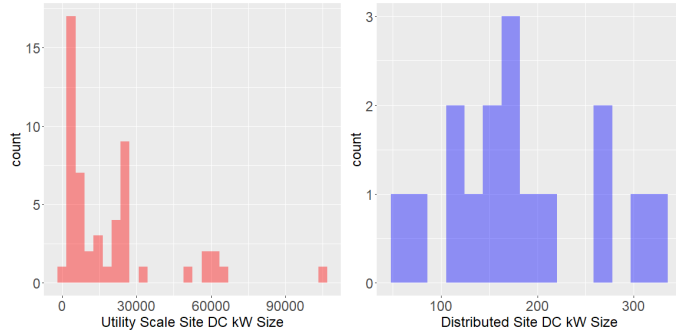


Fig. 1. Histograms of site size in DC kW for utility-scale (left) and distributed (right) sites used in this study.

112 *2) Particulate Matter Data:* Fine particulate matter, or
 113 PM2.5, is the main source of pollution from wildfires
 114 [20]. This particle count data is closely tracked at many
 115 sites throughout the U.S. and is openly accessible on the
 116 Airnow.gov website [15]. Airnow serves as a central repository
 117 for viewing and accessing U.S. Air Quality Index (AQI) data
 118 provided in partnership with several government agencies.
 119 There are many monitoring stations throughout the country
 120 that gather AQI data and report it to the Airnow website.
 121 Monitoring stations included in this analysis were identified
 122 based on their distance to the nearest solar PV site. If the
 123 distance between the solar PV site and closest PM2.5 mon-
 124 itoring station was greater than 30 miles, the solar PV site
 125 was removed from the analysis. Based on the locations of the
 126 selected solar PV sites, 16 PM2.5 monitoring stations were
 127 identified and used in this analysis. The mismatch between the

128 number of solar PV sites and PM2.5 monitoring stations is due
 129 to a single monitoring station being proximal to multiple solar
 130 PV sites. A sample of PM2.5 concentrations in the western
 131 U.S. on November 14, 2018 during the Camp Fire wildfire
 132 provide a glimpse of the spatial extent and heterogeneity in
 133 PM2.5 that can occur during these events (see Figure 2). The
 134 black triangle on the plot shows the fire's location. PM2.5
 135 monitoring stations are colored in correspondence with their
 136 average daily particle count, which is a function proximity to
 137 the fire. At least one monitoring station was found in each
 138 state containing a solar PV site.

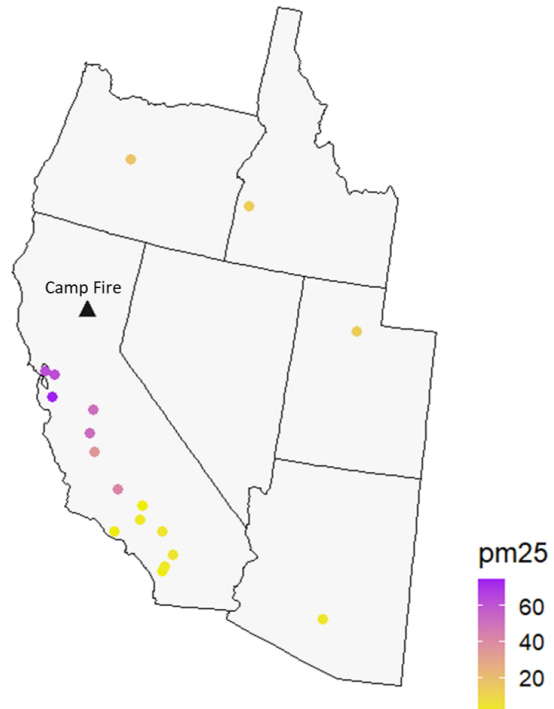


Fig. 2. Average daily PM2.5 concentration at monitoring stations during the Camp Fire Event on Nov. 14, 2018. Each location represents a PM2.5 station used in this study.

139 We obtain historical hourly PM2.5 data for the period
 140 April 2018 - July 2019 in units of $\mu\text{g}/\text{m}^3$ (micrograms per
 141 cubic meter of air) from each identified monitoring station to
 142 measure the impact of smoke. We assume that the PM2.5 data
 143 at the monitoring station is equivalent to the concentration at
 144 the PV solar site. A representative time series of PM2.5 at a
 145 solar PV site shows minimal increases in PM2.5 during the
 146 Mendocino Complex Fire but elevated concentrations during
 147 the Camp Fire (see Figure 3).

148 *3) Historical Weather Data:* The NASA Prediction of
 149 Worldwide Energy Resource (POWER) Project is a repository
 150 of global solar and meteorological data that is of general
 151 interest to the energy community [21]. For this project, we
 152 collected daily historical mean temperature at 2 meters (T),
 153 wind at 10 and 50 meters (W10M, W50M), precipitation (P),
 154 and insolation clearness index (CI) data at the solar PV site

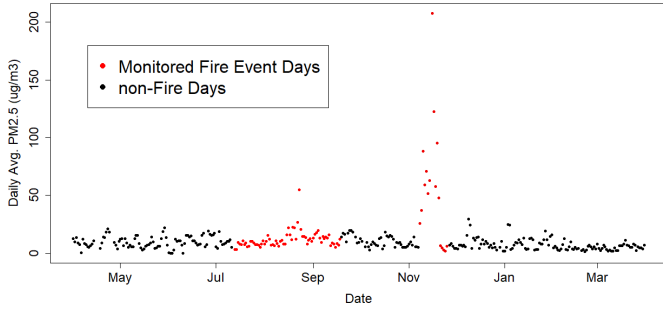


Fig. 3. Time series of PM2.5 for a solar PV site near the San Francisco Bay area in California.

155 for the time period of interest. We include these additional
 156 explanatory variables to help improve both predictive model
 157 fit as well as isolate the effects of the PM2.5 variable, which
 158 is of primary interest.

159 *B. Data Processing*

160 The data processing took place in two parts. First, all data
 161 was coerced into a consistent time scale. Then, the energy
 162 generation data was normalized to provide a common scale
 163 across all solar PV sites. The three datasets (i.e., solar PV
 164 energy generation, PM2.5 data, and weather data) were fused
 165 together to form a cohesive data panel. Additional details
 166 regarding the data processing are below.

167 *1) Time scale consistency:* The unprocessed production,
 168 weather, and PM2.5 data was available in two levels of tempo-
 169 ral precision. The PV site energy production and PM2.5 data
 170 were recorded hourly, whereas the NASA POWER weather
 171 data was available at the daily time scale. We chose the daily
 172 time scale to achieve temporal consistency across all three
 173 datasets.

174 For production data, daily values were obtained for each site
 175 through two steps. First, any negative hourly values were
 176 removed. The remaining hourly observations were then limited
 177 to only hours occurring between sunrise and sunset. The daily
 178 total energy production for the site was obtained by summing
 179 across all remaining hours for the day. Days where there was
 180 measured irradiance but no production for at least one hour
 181 during the middle of the day were removed from analysis.
 182 Additionally, there were four sites that consistently had ab-
 183 abnormally small production values even after aggregation; they
 184 were excluded from the study.

185 For the PM2.5 data, daily data was calculated as a weighted
 186 average. The weights were based on the theoretical clear sky
 187 direct normalized irradiance at each site. The hourly clear sky
 188 irradiance for each day is calculated for the exact location
 189 of the site using the *pvlib* python package [22]. Next, the
 190 hour is given a weight that is the percentage of the daily
 191 irradiance that occurs during the given hour. These weights
 192 are then used to calculate a daily weighted average of PM2.5
 193 for the site. This weighting scheme results in a daily average
 194 PM2.5 with each hour of PM2.5 data having an impact

195 on the daily average proportional to that hour's irradiance.
 196 Smoke that occurs during hours of no measured irradiance
 197 (e.g., nighttime) have no impact on daily average PM2.5
 198 calculations. Similarly, smoke that occurs during times of high
 199 irradiance (e.g., midday) have the largest impact on PM2.5
 200 daily averages. A sample time series of hourly irradiance and
 201 weighted PM2.5 shows periods of low and high irradiance and
 202 fluctuating levels of PM2.5 (see Figure 4). In this example the
 203 unweighted average PM2.5 measurement for that day is 51.83.
 204 However, the weighted irradiance average is 47.99. Days that
 205 have higher contrasts of smoke during the night and day will
 206 have larger differences in this calculation.

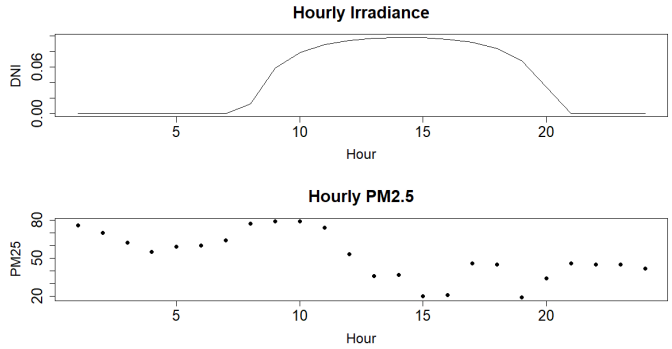


Fig. 4. Sample time series of hourly irradiance (top) and PM2.5 (bottom) data used to calculate the daily weighted average PM2.5 calculations.

207 The weighting process is applied to all days and sites used
 208 in this study. There is significant variability in the average
 209 daily PM2.5 for the region during the study period (see
 210 Figure 5). The two prominent fire events during this period
 211 result in elevated PM2.5 concentrations for the region. While
 212 the Mendocino Complex Fire had a longer duration than the
 213 Camp Fire, it has lower average PM2.5 concentrations.

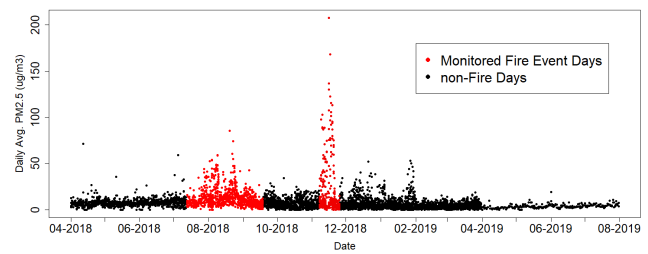


Fig. 5. Average daily PM2.5 concentration across all monitoring stations used in this study.

214 *2) Energy Production Normalization:* A normalization of
 215 the energy production data is needed due to the differing
 216 sizes of sites used in this study (see Figure 1). The daily
 217 IEC clear sky production is calculated for every site and
 218 day using the *pvOps* python package [23]. Each site's daily
 219 production is normalized by dividing the observed production
 220 by the IEC clear sky production. A sample hourly time series
 221 demonstrates the difference between the observed and IEC

222 clear sky energy production (see Figure 6). The normalization
 223 procedure results in all sites, regardless of size, having a
 224 production value on the same scale for analysis.

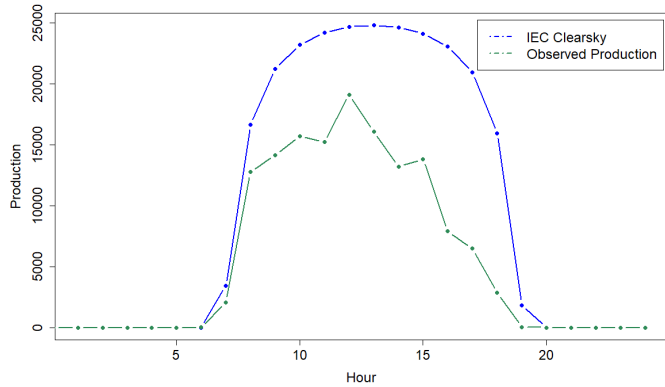


Fig. 6. Sample time series of observed & IEC clear sky energy production.

225 The normalization process resulted in some days being
 226 problematic. All days which had a normalized production
 227 greater than 1.2 (i.e., 120% of IEC clear sky) were removed
 228 from analysis. This threshold was based on discussions with
 229 industry and resulted in the removal of four sites that
 230 consistently had abnormally large normalized production values.
 231 There are additional abnormal production values in the data.
 232 However, we did not remove additional problematic data to
 233 minimize assumptions.

234 C. Data analysis

235 Regression models were the primary data analysis method
 236 used in this study. In particular, we focus on modeling the
 237 relationship between smoke (i.e., PM2.5) and solar PV pro-
 238 duction. All available data, across all sites, was included in the
 239 model analysis to have the largest data set possible to measure
 240 key relationships. Two quantitative methods were employed to
 241 assess model performance: R^2 , and the root mean square error
 242 ($RMSE$). An iterative process was used to consider different
 243 combinations of explanatory variables while attempting to
 244 maximize R^2 , minimize $RMSE$, and retain variables that
 245 were statistically significant (95% confidence interval).

246 III. ANALYSIS & RESULTS

247 A. Regression Model Selection

248 The initial regression model was based on regressing PM2.5,
 249 temperature at 2 meters, wind speed at 10 and 50 meters, pre-
 250 cipitation, and insolation clearness index. There is a seasonal
 251 component to solar PV production. The temperature variable
 252 was used to account for this as it tracked this variability
 253 closely. Some possible variable interactions were investigated.
 254 These interactions were excluded as they were found to be
 255 statistically insignificant.

256 There was still a large amount of variability in the data.
 257 A site-specific variable (i.e., a site adjustment factor) was
 258 introduced to improve model fit. This variable was significant

259 and improved model fit. However, it resulted in the model
 260 no longer capturing any temperature effects. As a result,
 261 temperature was therefore removed from the model in favor
 262 of the site adjustment variables. The significance of the site
 263 adjustment variable indicates that there are some inherent
 264 differences in production across sites, even after normalizing
 265 the production data.

266 The final selected model achieved $R^2 = .6732$, indicating
 267 that the model explains 67.32% of the variability in the daily
 268 production at the solar PV sites. In addition to the site adjust
 269 variables, PM2.5, insolation, precipitation, and wind speed
 270 were found to be statistically significant (see Table I for a
 271 summary of the final model). We only present a few site
 272 adjustment variables for illustrative purposes.

TABLE I
 REGRESSION MODEL PARAMETER SUMMARY. ONLY THREE SITE
 ADJUSTMENT PARAMETERS ARE INCLUDED FOR COMPARATIVE
 PURPOSES.

Parameter	Estimate	Std. Error	t value	P value
Intercept	0.0659	0.0073	9.0490	<2e-16
PM2.5	-0.0019	0.0001	-19.5190	< 2e-16
Insolation CI	0.8614	0.0066	131.3980	< 2e-16
Precipitation	-0.0030	0.0002	-12.3460	< 2e-16
Wind Speed 10M	0.1025	0.0026	39.6450	< 2e-16
Wind Speed 50M	-0.0710	0.0019	-36.6450	< 2e-16
Site C2S101	0.0393	0.0075	5.2110	< 2e-7
Site C2S106	0.0007	0.0076	0.0960	0.9235
Site C2S107	-0.0751	0.0076	-9.9380	< 2e-16

273 Separate parallel regression lines for every site have been
 274 incorporated. This site variable is specific to these sites, but
 275 it is not requirement to use the model for prediction. Two
 276 approaches can be taken. With no site information, a site effect
 277 of zero can be assumed. Alternatively, access to some site
 278 production information enables the site effect to be measured.

279 Model assumptions are satisfied based on residual analyses
 280 (see Figure 7). Studentized residuals are residuals where the
 281 model is fitted to all data except for that observation. The
 282 distance between the observed and the model's predicted value
 283 is calculated. This aids in preventing anomalous observations
 284 from pulling the model towards them and therefore reducing
 285 their residual value. The fitted versus residual plot should
 286 display no apparent trend (i.e., appear to be a random cloud
 287 of points) if the model fits the data well. Most points behave
 288 in this manner, but there appears to be a diagonal line
 289 cutting off the points on the left side of the plot. This line
 290 is associated with the zero cut-off for observed production
 291 and not a problematic trend. The Q-Q plot should roughly
 292 display as a straight line, and these results suggest that the
 293 normality assumption of the residuals has been satisfied. Thus,
 294 no transformations or additional variables are required to have
 295 confidence in model results.

296 The primary goal of this analysis was to measure the
 297 impact of smoke on solar PV energy production. Maximizing
 298 R^2 increases confidence in a model's ability to predict this
 299 relationship. The overall model ($R^2 = .6732$) is a good result
 300 as the weather predictors were not obtained at the site but

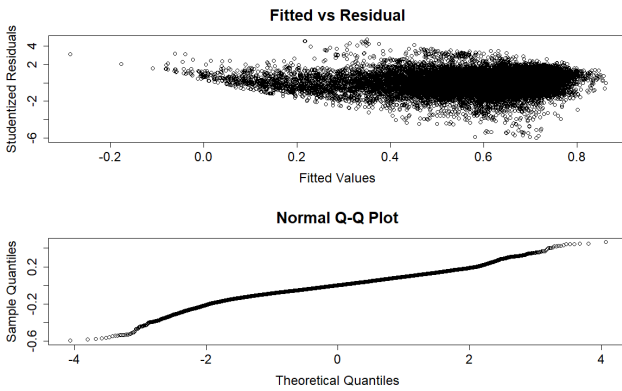


Fig. 7. Residual analysis plots.

rather come from satellite measurements. Additionally, the final selected model has $RMSE = 0.099$. This indicates that there will be, on average, an approximate difference of 0.099 normalized kWh ($\sim 10\%$ of daily site production) between the estimated and true daily energy generation for predicted observations. $RMSE$ appears to be significantly better than the R^2 . This is likely caused by a small portion of the data being significantly different than the model (outlier candidates). These outliers result in increased data variability not explained by the model, which more adversely effects the R^2 metric than the $RMSE$ metric.

B. Model Analysis

The PM2.5 variables regression parameter estimate is -0.0019 . Thus, as daily average PM2.5 increases by one $\mu\text{g}/\text{m}^3$, the normalized production is expected to decrease by approximately 0.0019. On days when PM2.5 reaches $50\text{--}200\mu\text{g}/\text{m}^3$, the model predicts a 9.4% to 37.8% reduction in normalized production, respectively. Similarly, normalized production is anticipated to decline as precipitation and wind speed at 50m increase by 0.0030 and 0.0710, respectively. Conversely, normalized production is predicted to increase by 0.8614 and 0.1025 due to a one unit increase in insolation and wind speed at 10m, respectively.

The site variables (only 3 of 68 displayed; see Table I)) indicate an adjustment factor for the linear model, and no change in the PM2.5 and weather parameter values. For example, site C2S101 (arbitrary ID), has an adjustment estimate of 0.0393, which indicates that normalized production for this site is expected to be 0.0393 higher than other sites. It should be noted that not every site correction is significant. In these cases, there is effectively no correction (zero effect).

A visual comparison between the observed normalized and predicted production data shows both clustering around a 1:1 fitted line as well as significant numbers of outliers (see Figure 8). There is a clear linear trend between predicted and observed values, but some additional trends are also present. There are a significant number of points in the lower right quadrant of the graph with high predicted values and low observed values. Some of these could be anomalies where

some production was not observed or some site operations resulted in reduced production. There are some days during which the model predicts negative production when production is observed to be near zero. Negative production is infeasible. These days are likely the result of rare events where several weather variables that all negatively impact production are observed simultaneously. In these instances, the model would round normalized energy production to zero.

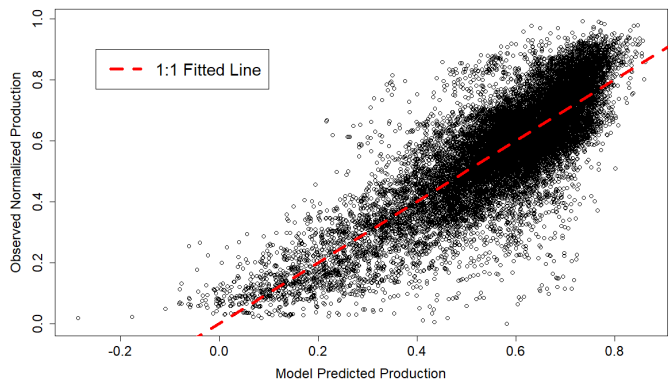


Fig. 8. Predicted versus observed normalized production across all sites used in this analysis.

A time series for the study domain provides a comparison between the observed normalized and predicted production data for sample site (see Figure 9). Additionally, this graphic displays both fire events in red. Overall, the predicted production follows the observed production well. There is one notable exception in late June where the observed production is quite lower than expected. There is a clear reduction in production during both of the fire events present in both the observed and predicted normalized production. The first fire event appears to have a more pronounced reduction in production in late August. This corresponds with the site's observed peak PM2.5. There is also a significant reduction in production during the Camp Fire event in November present in this graphic, this is in correspondence with the very high rates of PM2.5 during the month of November in 3. The high rates of variability in the normalized production after the Camp Fire event is due in large part to clouds and precipitation. There is a possible interaction between lower rates of precipitation leading up to and during fire events that could have some impact on solar production during this time which is not explored here.

IV. DISCUSSION

A statistical model can capture the basic relationship between air quality, which serves as a proxy for wildfire impacts, and the energy production of a nearby solar PV site. Additionally, while we find that PM2.5 plays a large role, other variables also factor in when it comes to capturing performance impacts during non-wildfire time periods, and our model can account for these changes. For example, the model is still able to capture the daily production fluctuations in the

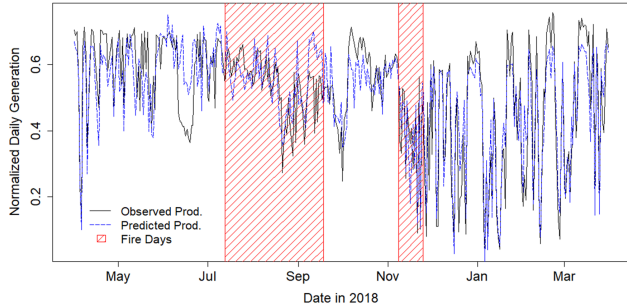


Fig. 9. Predicted versus observed normalized production for a solar PV site near the San Francisco Bay area in California.

377 days following the end of the fire event when PM2.5 levels
 378 have largely returned to normal.

379 There are several limitations to this analysis and possible
 380 next steps. In the data, there is no way to distinguish between
 381 either the impacts of smoke on production due to the blocking
 382 of solar irradiance or ash soiling on PV panels. This includes
 383 no ability to measure or determine the possible lingering
 384 effects of ash soiling after smoke has cleared, either on panels
 385 or other site instruments. Most of the smoke impact observed
 386 in this analysis is believed to come from smoke blocking
 387 solar irradiance. Several sites were removed from analysis for
 388 problematic data. Future work could refine the process for
 389 defining normal and abnormal behavior alike to remove only
 390 specific days as opposed to a site's full time series. Additional
 391 weather data or site-specific geographical features could be
 392 considered to further refine the model, both improving its
 393 predictive power and refining smoke impact quantification.
 394 Further testing of model performance could be done using
 395 site production validation data that was not used in fitting the
 396 model.

397 V. CONCLUSION

398 Wildfires are becoming increasingly common and increasing-
 399 ingly severe, requiring better planning for all levels of potential
 400 impact. One growing consideration is the impact of wildfire-
 401 induced pollution on solar PV production. We show here that
 402 high levels of PM2.5 in the atmosphere play a large role in
 403 disrupting energy production at affected PV sites, and we have
 404 developed a statistical model to better understand the strength
 405 of this relationship, as well as the degree to which other
 406 weather parameters factor affect PV energy generation. The
 407 regression model identifies a reduction in solar PV production
 408 between 9.4% to 37.8% on smokey days. This model can
 409 be used in conjunction with historical smoke data or smoke
 410 spread models to predict solar PV losses associated with
 411 wildfires for PV sites. Predicting losses can help with both
 412 long term prediction as well as short term emergency response
 413 planning. For advanced planning and operational support, this
 414 type of model can be combined with mature products that
 415 forecast smoke movement and air quality impacts to determine

416 which set of PV sites will be impacted by wildfire smoke and
 417 to what degree.

418 ACKNOWLEDGMENT

419 Sandia National Laboratories is a multimission laboratory
 420 managed and operated by National Technology & Engineering
 421 Solutions of Sandia, LLC, a wholly owned subsidiary of Hon-
 422 eywell International Inc., for the U.S. Department of Energy's
 423 National Nuclear Security Administration under contract DE-
 424 NA0003525. This paper describes objective technical results
 425 and analysis. Any subjective views or opinions that might
 426 be expressed in the paper do not necessarily represent the
 427 views of the U.S. Department of Energy or the United States
 428 Government. **SAND No. XXX**

429 REFERENCES

- [1] K.T. Weber et al. RECOVER: Geography of Wildfires Across the West. https://giscenter.isu.edu/research/Techpg/nasa_RECOVER/pdf/GeographyWildfires.pdf.
- [2] J.S. Schlosser et al. Analysis of aerosol composition data for western United States wildfires between 2005 and 2015: Dust emissions, chloride depletion, and most enhanced aerosol constituents. *Journal of Geophysical Research: Atmospheres*, 122(16):8951–8966, 2017.
- [3] A.L. Westerling, H.G. Hidalgo, D.R. Cayan, and T.W. Swetname. Warming and earlier spring increase western us forest wildfire activity. *Science*, 313(5789):940–943, 2006.
- [4] P.E. Dennison, S.C. Brewer, J.D. Arnold, and M.A. Moritz. Large wildfire trends in the western united states, 1984–2011. *Geophysical Research Letters*, 41(8):2928–2933, 2014.
- [5] K. O'Dell, B. Ford, E.V. Fischer, and J.R. Pierce. Contribution of wildland-fire smoke to us pm2. 5 and its influence on recent trends. *Environmental Science & Technology*, 53(4):1797–1804, 2019.
- [6] California Energy Commission. California Solar Energy Statistics and Data. https://ww2.energy.ca.gov/almanac/renewables_data/solar/index_cms.php#:~:text=In%202019%2C%20solar%20PV%20and,12%2C33820megawatts%2C%20are%20in%20California., 2021.
- [7] D. Feldman and R. Margolis. Q4 2019/Q1 2020 Solar Industry Update NREL/PR-6A20-77010. <https://www.nrel.gov/docs/fy20osti/77010.pdf>, 2020.
- [8] California Department of Forestry and Fire Protection. 2017 Wildfire Activity Statistics. https://www.fire.ca.gov/media/10059/2017_redbook_final.pdf, 2019.
- [9] K. Sun, L. Lu, J. Yu, Y. Wang, K. Zhou, and Z. He. Integrated effects of PM2.5 deposition, module surface conditions and nanocoatings on solar PV surface glass transmittance. *Renewable and Sustainable Energy Reviews*, 82:4107–4120, 2018.
- [10] I. Neher et al. Impact of atmospheric aerosols on photovoltaic energy production scenario for the sahel zone. *Energy Procedia*, 125:170–179, 2017.
- [11] H. Liu et al. The Impact of Haze on Performance Ratio and Short-Circuit Current of PV Systems in Singapore. *IEEE Journal of Photovoltaics*, 4(6), 2014.
- [12] M.H. Bergin, C. Ghoroi, D. Dixit, J.J. Schauer, and D.T. Shindell. Large reductions in solar energy production due to dust and particulate air pollution. *Environmental Science & Technology Letters*, 4(8):339–344, 2017.
- [13] J. Son, S. Jeong, H. Park, and C-E Park. The effect of particulate matter on solar photovoltaic power generation over the Republic of Korea. *Environmental Research Letters*, 15, 2020.
- [14] R.R. Cordero et al. Effects of soiling on photovoltaic (pv) modules in the atacama desert. *Scientific Reports*, 8(1):1–14, 2018.
- [15] U.S. Environmental Protection Agency. AirNow.gov - Home of the U.S. Air Quality Index. <https://www.airnow.gov/>, 2020.
- [16] CalFire. Ranch Fire (Mendocino Complex) Incident Report. <https://www.fire.ca.gov/incidents/2018/7/27/ranch-fire-mendocino-complex/4>, 2021.
- [17] CalFire. River Fire (Mendocino Complex) Incident Report. <https://www.fire.ca.gov/incidents/2018/7/27/river-fire-mendocino-complex/>, 2021.

482 [18] CalFire. Camp Fire Incident Report. <https://fire.ca.gov/incident/?incident=75daf80-f18a-4a4a-9a37-4b564c5f6014>, 2021.

483 [19] G.T. Klise. Pv reliability operations maintenance (pvrom) database: Data
484 collection & analysis insights [powerpoint]. Technical report, Sandia
485 National Lab.(SNL-NM), Albuquerque, NM (United States), 2015.

486 [20] D. Jaffe, W. Hafner, D. Chand, A. Westerling, and D. Spracklen.
487 Interannual variations in PM2. 5 due to wildfires in the Western United
488 States. *Environmental Science & technology*, 42(8):2812–2818, 2008.

489 [21] NASA. Prediction Of Worldwide Energy Resources (POWER). <https://power.larc.nasa.gov/>.

490 [22] W.F. Holmgren, C.W. Hansen, and M.A. Mikofski. pvlib python: a
491 python package for modeling solar energy systems. *Journal of Open
492 Source Software*, 3(29):884, 2018.

493 [23] T. Gunda, M. Hopwood, and H. Mendoza. pvOps – a python package
494 for PV operators & researchers. <https://pypi.org/project/pvops/>, 2021.

495

496